

INVESTIGATION OF THIRD BODY PROCESSES BY *IN VIVO* RAMAN TRIBOMETRY

Irwin L. Singer¹, S. David Dvorak², Kathryn J. Wahl¹

¹US Naval Research Laboratory, Code 6176

Washington, D.C. 20375-5342 USA

²Dept. of Mechanical Engineering Technology

University of Maine, Orono, ME 04469-5711 USA

ABSTRACT

A Raman tribometer has been used to study third body processes and friction during sliding against two low friction coatings: annealed boron carbide and Mo-S-Pb, a MoS₂-based coating. Reciprocating sliding tests were performed in either dry or humid air with transparent hemispheres (glass or sapphire) loaded against the coatings. Videos and Raman spectra of the sliding contact were recorded during the tests. For annealed boron carbide, friction was controlled by a mix of H₃BO₃ and carbon; for amorphous Mo-S-Pb, friction was controlled by MoS₂ generated by sliding. Friction changes in the former were correlated to the relative amount of the two materials; in the latter, the rise in friction was ascribed to a change in interfacial shear strength of MoS₂, inferred from the deformation of transferred debris particles. For both coatings, interfacial sliding was the dominant mode of velocity accommodation in the sliding interface.

1. INTRODUCTION

Friction is often treated as a two-body problem, in which the two counterfaces move against each other and a “magical” parameter – the friction coefficient – comes into being. Not so. At some scale, from atomically thin surface films to chunks of wear particles, third bodies play an important role in friction [1]. These “third bodies” are often born in the sliding contact, detach from one surface, transfer to the counterface and eventually agglomerate as macroscopically visible debris particles. When ejected from the contact, they are recognized as wear particles and written about extensively in friction and wear literature. When entrapped in the contact, they strongly influence the way the counterfaces accommodate sliding motion, the ‘velocity accommodation mode,’ but often go unnoticed because they are buried at the sliding interface.

One of the reasons that friction processes are not better understood is that the buried interface – where all the action takes place – is difficult to access experimentally. To study this interface, tribologists have traditionally had to separate the contacts before analyzing

them. This *ex situ* approach has provided useful clues to infer how third bodies form, what is their chemistry and structure, and how they participate in the sliding process. To prevent contamination, the chemistry of the interface can be evaluated by performing friction tests then separating and analyzing surfaces in a chamber with a well-controlled environment [2,3,4]. This *in situ* approach is necessary when the chemistry of surface films (nm thick) is important. The buried interface can also be accessed in real time by probing the sliding contact directly, via electrical [5], thermal [6], spectroscopic [7,8] or optical techniques [9,10,11,12]. When optical spectroscopy is combined with optical microscopy, this *in vivo* approach allows one to identify the composition of the sliding interface while watching third bodies form and move around the contact. The above four approaches are described in more detail by Donnet [13].

In this paper, we begin by reviewing some of our earlier *ex situ* studies on the friction behavior of dry sliding contacts. The studies, which identified third bodies found at various stages of sliding, allowed us to infer correlations between friction and third body processes. Next, we present preliminary results of *in vivo* studies of sliding behavior obtained with a tribometer designed to monitor the chemistry and morphology at the sliding contact during friction tests [14,15]. The tribometer sits below a microscope, which is connected to a video recorder and a Raman spectrometer; the microscope is focused on the sliding contact through a transparent hemisphere that is loaded against a coated substrate undergoing reciprocating sliding motion.

Friction tests were performed on annealed boron carbide and Mo-S-Pb, whose lubricating properties have been recently been investigated by *ex situ* techniques. Annealed boron carbide coatings have been shown to react with oxygen and moisture, producing two materials, boron oxide and carbon, both of which exhibit low friction coefficients in ambient air [16,17]. The low friction of boron oxide has been attributed to the boric acid (H_3BO_3) that forms when water vapor reacts with boron oxide [18]. Similarly, many forms of carbon provide low friction [19]. The low friction of amorphous Mo-S-Pb has been attributed to the third body MoS_2 films and debris formed during sliding [20]. Video recordings were used to identify the velocity accommodation modes during sliding, and Raman spectrometry to identify materials formed in the sliding contact. Correlations of third bodies and friction behavior will be presented.

2. REVIEW OF *EX SITU* STUDIES ON ROLE OF THIRD BODIES

Over the past fifteen years, we have seen third body effects in virtually every investigation of sliding behavior of wear resistant coatings and surface treatments. We have shown that films and particles transfer to and from counterfaces, and have identified compositions and phases of many of these third bodies [21,22]. In our studies, friction and

wear tests have been carried out at relatively low speeds, typically 1 - 100 mm/s, with a sphere vs. flat geometry at high normal contact stresses, 0.5 - 1.5 GPa, in both unidirectional and reciprocating sliding. Surface topography, chemistry and microstructure are characterized before and after wear tests [23] and, more recently, by *in situ* triboscopy [24].

How do third bodies form? With many treated surfaces, such as ion-implanted steels [25] and coatings, such as TiN [26], TiC [27] and MoS₂ [28], third bodies begin with films that form on the surface, e.g., Ti oxides on TiN and TiC. Although sliding removes the films, subsequent films can grow if the environment provides reactive gases like oxygen [29] or H₂S [30]. These films become third bodies by detaching from the surface. Recently we have identified, using cross-section TEM, an atomic-scale detachment process on amorphous, ion-beam deposited Mo-S-Pb coatings [31,32]. It appears that sliding transformed the amorphous surface to basal-oriented MoS₂ platelets, from one to several layers thick, which subsequently delaminated and transferred to the counterface. Although transfer films are sometimes very thin, perhaps only a monolayer or so thick, they can be detected on counterfaces by Auger electron spectroscopy and other surface-sensitive spectroscopies long before wear is detected on the track [33,34].

What are the chemistry and structure of the third bodies? Although transfer films originate from a "parent" material, they do not always have the same phase or composition as the parent. The transformation of amorphous Mo-S-Pb to crystalline MoS₂ layers is one example. More complicated tribochemical reactions between ambient gases and rubbing counterfaces can also take place [28]. While Al₂O₃ (sapphire) sliding against TiN and TiC gave the expected TiO₂ (rutile) phase, a steel counterface produced ternary and quaternary phases [26,27]; the same was true of transfer films generated on MoS₂ coatings [35,36]. Compelling evidence for tribochemical control of friction and wear has been demonstrated by carrying out *in situ* friction tests at controlled gas pressures in a multi-analytical UHV chamber [37]; further evidence has recently been reported by Grossiord et al. [38] on boundary lubricant films analyzed in the same chamber by ion-sectioning wear scars produced *in situ*.

How third bodies participate in the sliding process has been examined most effectively in studies of three solid lubricant coatings, diamond-like carbon (DLC), MoS₂ and Mo-S-Pb. Unlike hard coatings and implantation treatments that give low friction for only short durations, both DLC [39,40] and MoS₂ [41] can give a million or more cycles of steady, low friction sliding before failing. However, like most wear-resistant coatings, both run on transfer films generated in the sliding contact by solid-solid and gas-solid reactions [36,42]. The fact that coatings only hundreds of nm thick can give such long life suggests that sliding takes place between transferred MoS₂ and the wear track on the MoS₂ coating. This was confirmed recently by Descartes, who performed *in vivo* optical microscopy of dry sliding

contacts [43]. Friction coefficients of DLC, MoS₂ and Mo-S-Pb coatings are generally lower ($\mu < 0.1$) than those obtained from conventional hard coatings ($\mu > 0.1$); moreover, they are very sensitive to contact pressure. In dry environments, friction coefficients of DLC [44], MoS₂ [45] and Mo-S-Pb [20] can depend on the load, L , i.e., they do not obey Amontons' Law; this behavior is consistent with the relationship $\mu = S_i / P$, in which “ S_i ” is an interfacial shear strength and “ P ” is the elastic contact pressure, where in an elastically-loaded contact, $P \propto L^n$ where $1/3 < n < 1/2$, depending on counterface geometry. MoS₂-based coatings continue to provide low friction even as the original coating thickness approaches zero; low friction is sustained by transferring films from third body reservoirs [46] to protect worn spots in the sliding contact [24]. Why some coatings form reservoirs and, thereby, give long life, while others eject the wear debris and fail early, is not well understood [47].

In summary, third bodies play an important role in the friction coefficient of low friction, wear resistant materials in dry sliding contact. They can reduce friction by forming transfer films, or can increase it by cluttering wear tracks with debris. Transfer films accommodate motion through interfacial sliding and by deformation processes; they also extend life of sliding contacts by forming third body reservoirs and replenishing, thereby healing, wear tracks with slippery material. Third bodies, however, are not simply small pieces of the parent wear track. They are films and particles synthesized at high stress in the contact by tribochemical processes. Perhaps we should be most surprised that they often take on compositions similar to those predicted by equilibrium thermochemical reactions. Hence, if we wish to design long-lived tribomaterials, we must have a more fundamental understanding of third bodies and third body processes. And that requires *in vivo* tribometry.

3. EXPERIMENTAL

The *in vivo* tribometer was built around a Renishaw System 1000 Raman microprobe, which consists of a low-power (25 mW) Argon laser (514.5 nm) excitation source, a holographic spectrometer, and an Olympus BH-2 microscope. The Raman system has a lateral spatial resolution of 2 μm and a spectrometer resolution of 1 cm^{-1} . A custom-built reciprocating stage was designed to fit underneath the optics of the microscope. Friction was measured by a piezo sensor mounted below the sample stage. Computer-aided data acquisition recorded both average and spatially resolved friction data. During friction testing, the optical microscope could be used either to observe the sliding contact or to perform micro-Raman spectroscopy. Observations were made using a video camera and recorded on VHS tape at 30 frames/s. Still images were obtained from the videotape. Raman spectra typically took between 5 and 10 cycles to obtain.

The annealed boron carbide coating was prepared by annealing a rf-magnetron-sputtered boron carbide coating at 800°C for about 15 min [17]. The Mo-S-Pb coating was

grown by ion beam deposition (IBD) on a hardened steel substrate [20,48]. Friction tests were performed in air at room temperature. Sliding speed was 1 mm/s over a track length from 4 - 6 mm. The hemispheres, , were loaded to against the coating. For the boron carbide study, a sapphire hemisphere, 6.35mm diameter, was loaded to 6.4N; for the Mo-S-Pb study, a glass hemisphere, 12.7mm diameter, was loaded to 24N.

4. RESULTS

4.1 Annealed boron carbide coating

Figure 1 shows a typical friction coefficient vs. cycle curve obtained with a sapphire hemisphere sliding against the annealed boron carbide coating on an Inconel substrate. The friction coefficient started out at about 0.08. It climbed slowly to about 0.10 over 400 cycles, then rose more rapidly to about 0.22 from cycle 450 to 800, and finally dropped to about 0.20. By contrast, a similar test of sapphire against uncoated inconel gave a much higher friction coefficient, between 0.6 and 0.8.

In vivo Raman spectra taken at selected cycles during the friction test are shown as insets in Fig. 1; the cycles at which the spectra were taken are indicated by the three circles on the friction curve. The peaks topped with an “x” are those of the sapphire hemisphere and

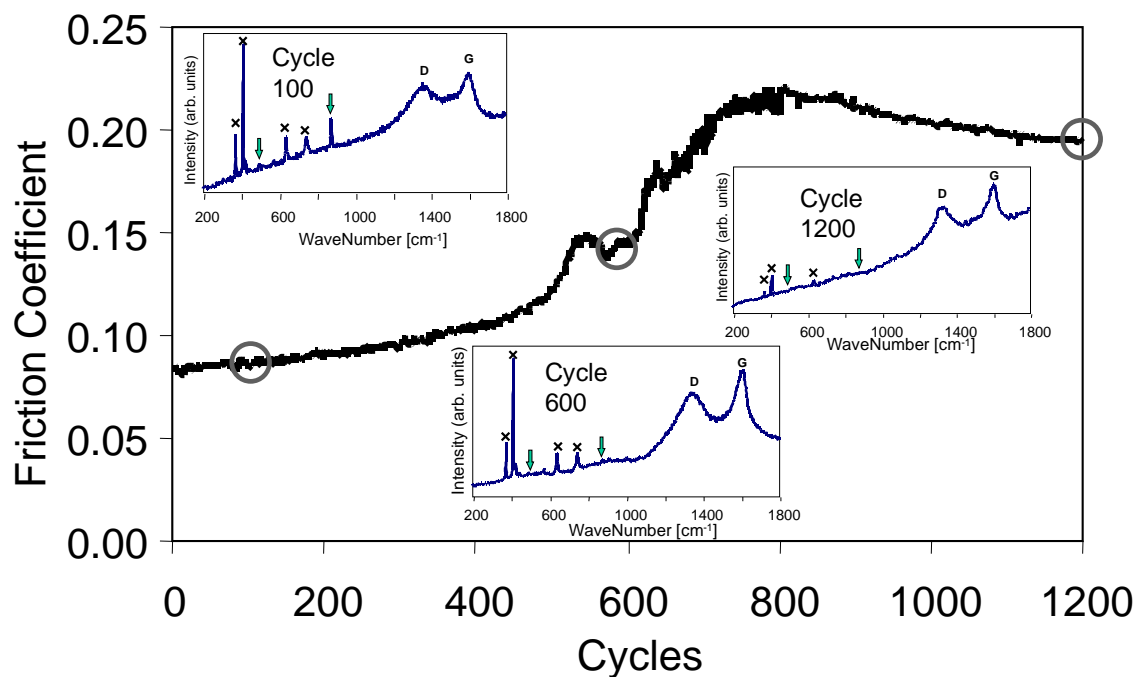


Fig. 1. Friction coefficient vs. cycles of annealed boron carbide coating on inconel. Circles indicate cycles during which *in vivo* Raman analysis was performed. Insets are the Raman spectra. Peaks topped with x are those of sapphire; peaks with arrow are those of boric acid.

will be ignored. The spectrum (Cycle 100), obtained at the beginning of low-friction ($\mu = 0.08$) sliding, shows peaks of H_3BO_3 (topped by ‘down arrows’) and two others that correspond to the D and G bands of carbon; the latter bands are found in many types of carbon films with nanoscale or amorphous structures, including graphitic carbon, amorphous carbon and DLC [49,50]. The second spectrum (Cycle 600), taken at a friction coefficient of about 0.15, shows that the carbon peaks became more pronounced, while the H_3BO_3 peaks disappeared. The third spectrum (Cycle 1200), taken when the friction coefficient leveled off at 0.20, also shows much larger carbon intensities (relative to sapphire), and, again, no H_3BO_3 . Post-test, ex-situ, Raman analysis of the separated contacts showed strong carbon peaks on both surfaces, whereas areas immediately adjacent to the contact still contained H_3BO_3 .

The *in vivo* Raman tribometry results of Fig. 1 allow us to correlate the low friction behavior of a coating with third body materials detected inside a sliding contact. The lowest friction coefficient, $\mu = 0.08$, was observed when both H_3BO_3 and carbon were in the contact; this value was slightly higher than $\mu = 0.06$ obtained in a similar test against a H_3BO_3 coating [14]. As the H_3BO_3 disappeared from the contact and the carbon intensity increased, the friction coefficient rose to 0.2. Friction coefficients of 0.15-0.20 are consistent with the values for several forms of carbon in ambient air [51]. These correlations confirm similar inferences drawn by Erdemir [16] from *ex situ* studies of the same coating.

The results also suggest that the friction coefficient for this mixture can be written as the sum of the friction coefficients from two third body contributions:

$$\mu = \alpha\mu_1 + (1-\alpha)\mu_2$$

where subscripts 1 and 2 here refer to H_3BO_3 and carbon and α and $(1-\alpha)$ are the contributions of the two materials, respectively (e.g., as could be determined by ratios of Raman peak intensities). Furthermore, the friction behavior of these materials was tribologically-friendly: as sliding removed the lower friction H_3BO_3 from the contact, the carbon provided a backup solid lubricant, albeit at a slightly higher value than H_3BO_3 alone. It is not clear why the slipperier material (H_3BO_3) initially controlled friction. Perhaps it segregated to the interface; or perhaps the higher friction carbon was either buried below the interface or ejected from the contact. The use of more than one lubricant phase to maintain low friction coefficients has been exploited [52,53] to design adaptive solid lubricant coatings, e.g., coatings made up of materials that are either lubricating or become lubricating during sliding. When one phase outlives its usefulness, for example, at a given temperature or in a given environment, a second lubricating phase takes over.

In summary, *in vivo* Raman tribometry demonstrated that two third body materials, H_3BO_3 and carbon, were responsible for the low friction sliding on annealed boron carbide, and the rise in the friction coefficient correlated directly with the loss of the lower friction material, H_3BO_3 , from the sliding contact.

4.2 Mo-S-Pb coating

Figure 2 shows a typical friction coefficient vs. cycle curve obtained with a glass hemisphere sliding against a Mo-S-Pb coating, first in dry air (RH < 1%), then humid air (50% RH), and finally back to dry air. After a short run-in period, the friction coefficient leveled out at about $\mu = 0.05$ in dry air. At cycle 645, the humidity was increased. The friction increased as the humidity rose, reaching a steady value of about 0.17. The humidity was then decreased at cycle 812 to RH < 1%, and again the friction tracked the humidity, returning to its previous level.

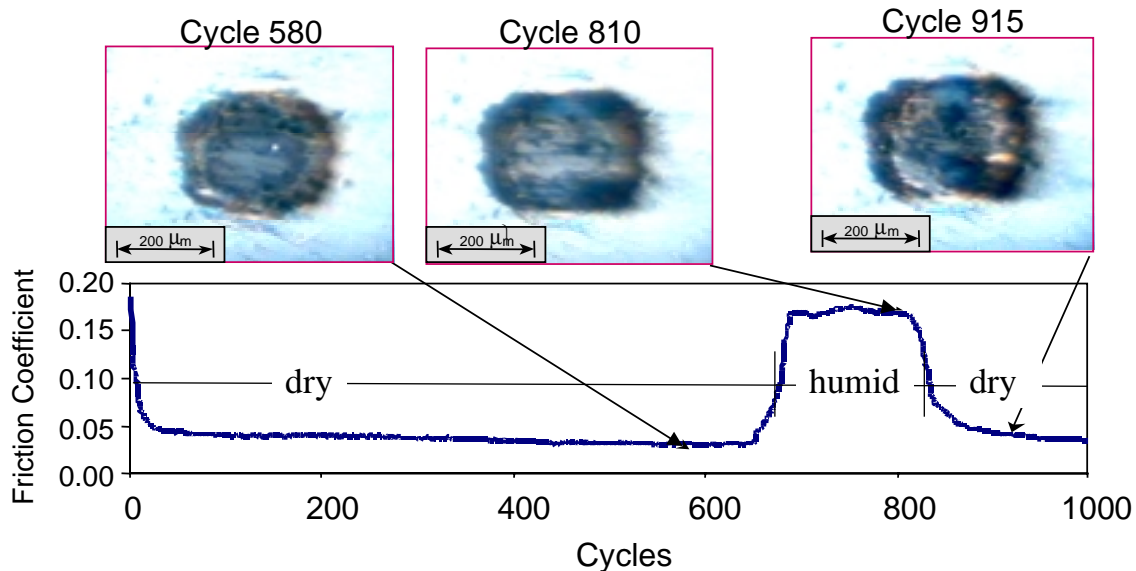


Fig. 2. Friction coefficient vs. cycles of Mo-S-Pb coating during dry, humid (RH = 50%) then dry sliding. Insets show *in vivo* images of sliding contact.

Figure 2 also shows single-frame images (from videotapes) of the contact zone before, during and after the humidity increased. As sliding progressed (in dry air), first a thin transfer film then particulate debris attached to the contact area of the hemisphere (not shown); later, thicker, compact pads of debris formed at the leading/trailing (right and left) edges of the contact. A few debris particles also adhered to the coating, as evident by their passage across the hemisphere at the sliding speed (1 mm/s). The pattern of transfer film and debris buildup in these *in vivo* images is similar to buildup observed *ex situ* in similar studies [20,32].

Moreover, the most prominent and constant observation was that the relative motion between the film/debris covered hemisphere and the coating surface took place by interfacial sliding.

However, as the humidity rose, some of the debris attached to the contact area of the hemisphere began to extrude - moving at speeds up to 3% of the sliding speed at highest humidity. In addition, loose debris appeared to be swept up from the track and collected at the leading/trailing edge of the contact, feeding additional debris into the contact. Nonetheless, most of the relative motion across the contacting surfaces at 50% RH was accommodated by interfacial sliding. Gradually, as the humidity and friction coefficient fell, the debris – still attached to the hemisphere – became stationary again, and all of the motion was accommodated by interfacial sliding. As seen in Fig. 2, the amount of debris in the contact remained similar through much of the test.

Raman spectra were taken *in vivo* at all stages of the test. Initially, the spectra showed only broad peaks from the glass hemisphere and the amorphous film. Within 100 cycles, two peaks characteristic of MoS₂ appeared and increased in intensity with increasing cycles; similar results were seen in earlier *ex situ* Raman analysis of the separated counterfaces [20,32]. Furthermore, no other peaks could be detected, before, during or after humidity exposure.

The earlier *ex situ* Raman studies suggested two reasons why amorphous Mo-S-Pb coatings had similar friction behavior to MoS₂ coatings. First, Mo-S-Pb, like MoS₂, ran on third body MoS₂ inside the contact [20,32]. The present study shows conclusively that MoS₂ was present in the contact **during** sliding. Secondly, in both cases, sliding occurred between a MoS₂ transfer film and MoS₂ at the surface of the coating, i.e., by interfacial sliding. Others [54,55] have reported that friction was controlled by shear properties of MoS₂ grains, themselves. The visual evidence here indeed shows that, in dry sliding, velocity was accommodated predominantly by interfacial sliding and not intergranular shear of the coating material or its debris. Hence, the low friction coefficient in both coatings was controlled by the interfacial ‘shear stress’ associated with interfacial sliding, i.e., $\mu = \mu_i = S_i/P$; for MoS₂ and Mo-S-Pb in dry air, the interfacial shear strength has been determined to be about 25 MPa [45,20].

With the addition of moisture, the friction rose by a factor of 3 to 4 and debris in the contact began to extrude, although most of the velocity was accommodated by sliding at the interface. Increases in friction of MoS₂ by this amount are well documented [56]. Some have speculated that the rise is due to composition changes such as MoS₂ converting to molybdenum oxides or hydroxides [56] Here we could detect no other phases, and if MoO₃ debris had been present, Raman spectra would have shown it [57]. Instead we suggest that the friction rise was more likely due to an increase in the interfacial shear strength as follows: as moisture condensed on the MoS₂ wear track, S_i increased, hence $\mu_i \propto S_i$ increased. As $\mu_i \propto S_i$

approached the value of the shear strength of MoS₂ debris particles, the debris began to shear and extrude. This explanation is consistent with the friction studies of Uemura et al. [58], which showed that the interfacial shear strength of MoS₂ sliding against MoS₂ is 2 to 3 times lower than the shear strength of MoS₂ crystallites. This mechanism can account for both the increased friction coefficient and deformation of the debris. An alternative mechanism, that the shear strength of debris particles in the contact decreased as the humidity increased, is less likely because the time scales at which the deformation behavior changed were very short (<< 1 minute). We plan to examine this issue in more detail in the future.

In summary, *in vivo* Raman tribometry identified several third bodies and the velocity accommodation modes associated with the friction coefficient of Mo-S-Pb coatings. In dry air, friction was controlled by interfacial sliding between the wear track on the coating and the transfer film (with attached debris) of MoS₂ on the hemisphere. In humid air, the rise in friction coefficient from 0.04 to about 0.15 caused a second velocity accommodation mode to appear: shear/extrusion of attached debris. In both cases, Raman could detect only MoS₂ in the contact, indicating that the friction changes were not due to formation of oxidized third body particles; rather, if a chemical reaction did take place, it most likely increased the interfacial shear strength during sliding.

5. Summary and Conclusions

In vivo analysis of the sliding contact between transparent hemispheres and two solid lubricant coatings clearly showed that third bodies play a major role in friction behavior. Several third body processes were identified and correlated with friction coefficients:

1. With both annealed boron carbide and amorphous Mo-S-Pb coatings, *in vivo* Raman detected third body materials: H₃BO₃ and carbon in the former; MoS₂, formed during sliding, in the latter. The low friction coefficients measured were attributed to the presence of these materials in the sliding contact.
2. With annealed boron carbide, the rise in the friction coefficient correlated with the mixture of third body materials (H₃BO₃ and carbon) in the contact. However, with Mo-S-Pb, the rise in the friction coefficient could not be attributed directly to a new third body material; rather, it was associated with a change in velocity accommodation mode. We speculated that the mode change was due to an increase in the interfacial shear strength of MoS₂, which eventually caused the MoS₂ debris to shear.
3. Interfacial sliding was the dominant mode of velocity accommodation in the sliding interface of the two low friction coatings.

4. Finally, it was demonstrated that *in vivo* Raman tribometry allows tribologists to visualize interfacial dynamics and identify near surface chemistry. This technique opens a new window on the buried sliding interface.

ACKNOWLEDGMENTS

The authors wish to thank Dr. Ali Erdemir for samples and useful conversations, Bob Bolster and April Coates Brabant for assistance with the design, construction and programming of the tribometer, ONR for funding the research. We also acknowledge the contributions of our many collaborators on third body research: R. Jeffries, S. Fayeulle, P. Ehni, R. Bolster, J. Wegand, L. Seitzman, Th. LeMogne, J.M. Martin, Ch. Donnet, M. Belin and D. Dunn. This research was performed while one of the authors, S.D. Dvorak, was at NRL on an ASEE Post-Doctoral Research Fellowship.

REFERENCES

1. M. Godet, *Wear* **100** (1984) 437; Y. Berthier, M. Brendle and M. Godet, *STLE Tribol. Trans.* **32** (1989) 490.
2. D.H. Buckley, *Surface Effects in Adhesion, Friction, Wear and Lubrication* (Elsevier, Amsterdam, 1981) Chap. 6.
3. J.M. Martin and T. Le Mogne, *Surf. Coat. Technol.* **49** (1991) 427.
4. I.L. Singer, T. Le Mogne, C. Donnet, and J.M. Martin, *J. Vac. Sci. Technol. A* **14** (1996) 38.
5. M. Belin and J.M. Martin, *Wear* **156** (1992) 151.
6. S. Bair, I. Green and B. Bhushan, *J. Tribology* **113** (1991) 547.
7. P.M. Cann and H.A. Spikes, *Tribology Transactions* **34** (1991) 248.
8. C.U Cheng and P.C. Stair, *Tribology Letters* **4** (1998) 163.
9. Y. Berthier, M. Godet and M. Brendle, *Tribology Transactions* **32** (1989) 490.
10. H. Sliney, *ASLE Trans.* **21** (1977) 109.
11. A. Jullien, M.H. Meurisse, Y. Berthier, *Wear* **194** (1996) 116.
12. J.N. Israelachvili and D. Tabor, *Wear* **24** (1973) 386.
13. C. Donnet, *Handbook of Surface and Interface Analysis*, J.C. Riviere, S. Myhra (eds.), (Marcel Dekker, Inc., 1998) Chapter 16, pp. 697-745.
14. S.D. Dvorak, K.J. Wahl and I.L. Singer, International Conference on Metallurgical Coatings and Thin Films (ICMCTF), San Diego, CA, 27 April 12-16 1999; to be published.
15. S.D. Dvorak, K.J. Wahl and I.L. Singer, 217th National Meeting of the American Chemical Society, Anaheim, CA, 21-25 March 1999; to be published.
16. A. Erdemir, C. Bindal, C. Zuiker and E. Savrun, *Surf. Coat. Technol.* **86-87** (1997) 507.
17. A. Erdemir, O. L. Eryilmaz, and G. Fenske, *Surf. Eng.* **15** (1999) 291.

18. A. Erdemir, G.R. Fenske, R.A. Erck, F.A. Nichols, D.E. Busch, *Lubr. Eng.* **47** (1991) 169.
19. J.K. Lancaster, *Tribology Int.* **23** (1990) 371.
20. K.J. Wahl, L.E. Seitzman, R.N. Bolster, and I.L. Singer, *Surf. Coat. Technol.* **73** (1995) 152.
21. I.L. Singer, *Langmuir* **12** (1996) 4486.
22. I.L. Singer, *MRS Bulletin* **23(6)** (1998) 37.
23. I.L. Singer, *Appl. Surf. Sci.* **18** (1984) 28.
24. K.J. Wahl, M. Belin, and I.L. Singer, *Wear* **214** (1998) 212.
25. S. Fayeulle and I.L. Singer, *Mater. Sci. Eng.* **A115** (1989) 285.
26. I.L. Singer, S. Fayeulle, and P.D. Ehni, *Wear* **149** (1991) 375.
27. S. Fayeulle and I.L. Singer, *Wear Particles: Cradle to Grave*, 18th Leeds-Lyon Symposium on Tribology, Tribology Series, 19, edited by D. Dowson, C.M. Taylor, M. Godet (Elsevier, GB, 1992) pp. 293-300.
28. I.L. Singer, *Surf. Coat. Technol.* **49** (1991) 474.
29. M.D. Sexton and T.E. Fischer, *Wear* **96** (1984) 17.
30. I.L. Singer, Th. Le Mogne, Ch. Donnet, and J.M. Martin, *J. Vac. Sci. Technol.* **14** (1996) 38.
31. D.N. Dunn, K.J. Wahl and I.L. Singer, *Fundamentals of Nanoindentation and Nanotribology*, edited by N.R. Moody, W.W. Gerberich, S.P. Baker, N. Burnham, (Mater. Res. Soc. Proc. 522, Pittsburgh, PA, 1998) pp. 451-456.
32. K.J. Wahl, D.N. Dunn and I.L. Singer, *Wear* **230** (1999) 175.
33. P.D. Ehni, and I.L. Singer, *New Materials Approaches to Tribology: Theory and Applications*, edited by L.E. Pope, L. Fehrenbacher and W.O. Winer, (Mater. Res. Soc. Proc. 140, Pittsburgh, PA, 1989) pp. 245-250.
34. K.J. Wahl, L.E. Seitzman, R.N. Bolster and I.L. Singer, *Surf. Coat. Technol.* **73** (1995) 152.
35. S. Fayeulle, P.D. Ehni and I.L. Singer, *Surf. Coat. Technol.* **41** (1990) 93.
36. S. Fayeulle and I.L. Singer, and P.D. Ehni, in *Mechanics of Coatings*, edited by D. Dowson, C.M. Taylor and M. Godet (Elsevier, Oxford, 1990) p. 129.
37. I.L. Singer, T. Le Mogne, Ch. Donnet and J.M. Martin, *Tribol. Trans.* **39** (1996) 950.
38. C. Grossiord, J.M. Martin, T. Le Mogne and T. Palermo, *Tribology Lett.* **6** (1999) 171; C. Grossiord, J.M. Martin, T. Le Mogne, K. Inoue and J. Igarashi, *J. Vac. Sci. Technol. A* **17** (1999) 884.
39. K. Enke, H. Dimigen and H. Hübsch, *Appl. Phys. Lett.* **36**, 291 (1980); K. Enke, *Thin Solid Films* **80** (1981) 227.
40. A. Grill, *Wear* **168** (1993) 143.
41. M. Suzuki, *Wear* **218** (1998) 110.
42. S. Miyake, S. Takahashi, I. Watanabe and H. Yoshihara, *ASLE Trans.* **30** (1987) 121; I. Sugimoto and S. Miyake, *Appl. Phys. Lett.* **56** (1990) 1868.
43. S. Descartes, Doctoral Thesis, INSA de Lyon, Lyon, France, October 1997.
44. I.L. Singer, in *Fundamentals of Friction*, edited by I.L. Singer and H.M. Pollock

- (Kluwer Academic Publishers, Dordrecht, 1992) p. 237.
45. I.L. Singer, R.N. Bolster, J. Wegand, S Fayeulle and B.C. Stupp, *Appl. Phys. Lett.* **57** (1990) 995.
 46. K.J. Wahl and I.L. Singer, *Trib. Lett.* **1** (1995) 59.
 47. K.J. Wahl, D.N. Dunn, and I.L. Singer, *Wear* **237** (2000) 1.
 48. R.N. Bolster, NRL Memorandum Report, NRL/MR/6176-92-7135 (1992).
 49. R.J. Nemanich and S.A. Solin, *Phys. Rev. B* **20** (1979) 392.
 50. J. Robertson, *Adv. Phys.* **35** (1986) 317.
 51. C. Donnet, *Surf. Coat. Technol.* **80** (1996) 151.
 52. C. DellaCorte and H.E. Sliney, *ASLE Trans.* **30** (1987) 77.
 53. J.S. Zabinski, M.S. Donley, V.J. Dyhouse, and N.T. McDevitt, *Thin Solid Films* **214** (1992) 156.
 54. See W.O. Winer, *Wear* **10** (1967) 422.
 55. P.D. Fleischauer and R. Bauer, *Tribol. Trans.* **31** (1988) 239.
 56. A.R. Lansdown, *Molybdenum Disulphide Lubrication*, (Elsevier, Amsterdam, 1999) pp. 56-58; 79-85.
 57. N.T. McDevitt, M.S. Donley, and J.S. Zabinski, *Wear* **166** (1993) 65.
 58. M. Uemura, K. Okada, A. Mogami and A. Okitsu, *Lubr. Eng.* **43** (1987) 937.